December 1979 LRP 161/79

NUMERICAL MODELS FOR THE QUASILINEAR EVOLUTION OF CURRENT-DRIVEN ION-ACOUSTIC TURBULENCE

K. Appert and J. Vaclavik

Numerical Models for the Quasilinear Evolution of Current-Driven Ion-Acoustic Turbulence

K. Appert and J. Vaclavik

Centre de Recherches en Physique des Plasmas

Association Euratom - Confédération Suisse

Ecole Polytechnique Fédérale de Lausanne

CH-1007 Lausanne / Switzerland

ABSTRACT

We consider the temporal evolution of ion-acoustic turbulence induced by a constant current in a two-temperature plasma ($T_e >> T_i$). The evolution is described by a quasilinear model which includes resonant and nonresonant wave-particle interactions. The resonant interaction, through its local features in velocity space, requires discrete particle distribution functions which may respond locally in the resonant region. We choose a finite element discretization and show, by comparison with the frequently used approach of evolving Maxwellian distributions, that the latter may produce both quantitatively and qualitatively erroneous results. We then show that the high energy ion tail, for whose formation the nonresonant interaction is essential, may quench the ion-acoustic instability in the way proposed by Dum and co-workers when interpreting their particle-in-cell simulation results.

../2

I. INTRODUCTION

Current driven ion-acoustic turbulence and the anomalous resistivity related to it has been one of the most fundamental problems of plasma and controlled fusion physics as well as of astrophysics in the last two decades. Experimental work is currently being done on two different heating schemes for controlled fusion devices which rely, at least in part, upon the anomalous resistivity due to ion sound turbulence. On the one hand, it has been shown[1,2] that large toroidal devices might be turbulently heated through a skin layer by an alternating electric field. On the other hand, experiments on relativistic beam heating of plasmas indicate that the return current of drifting plasma electrons gives rise to ion-sound turbulence which enhances the dissipation of the beam energy.[3,4] The ion-sound turbulence might also be important in laser fusion where it could limit the electron heat flux to anomalously low values.[5] As far as anomalous resistivity under astrophysical conditions is concerned, it appears that it must usually be connected with ion-sound turbulence.[6] Fast plasma heating in chromospheric flares, for instance, and in the vicinity of pulsars may be explained in this way.[6] Moreover, the anomalous dissipation due to ion-sound turbulence may play an important role in the formation of collisionless shock waves.

../3

Various laboratory[3,4,7] and computer simulation experiments[8,9], as well as analytical considerations[10], indicate that high energy ions are an important feature of ion-acoustic turbulence. Up to now, theories in which high energy ions are considered, suffer from serious drawbacks. It is, for example, difficult to understand how the one-dimensional coherent trapping theory proposed by Manheimer and Flynn[11] could be applied to a basically multidimensional spectrum as it is seen in experiments.[8,12] On the other hand, in the theories involving resonance broadening[13-15], which is a higher order effect in the framework of weak turbulence theory, the most important lower order effect, namely local quasilinear flattening, is not taken into account. In these theories the ion tails are assumed to be Maxwellian and therefore cannot exhibit local quasilinear flattening.

The objective of the present paper is to investigate numerically the temporal evolution of ion-acoustic turbulence driven by a constant current. Using different physical models and different numerical approximations, we will be able to draw conclusions concerning their relevance and their applicability. In Sec. 2 the basic equations are given. In Sec. 3 we assume Maxwellian distribution functions allowing the temperatures and a discretized wave spectrum to evolve in time according to quasilinear equations. These equations may or may not include nonresonant wave-particle interactions. In Sec. 4 we replace first the Maxwellian ion distribution by a one-dimensional finite element distribution, which allows for local quasilinear effects, and show that the results differ qualitatively from those in Sec. 3. The case of a two-dimensional discretized electron

../4

distribution function[18] is discussed afterwards. A scaling law for the ion tail formation by nonresonant wave-particle interaction is obtained in Sec. 5 on the basis of a one-dimensional model. The model includes Maxwellian electrons, finite element ions and finite element waves. In using this model, however, no saturation is obtained. The saturation is the topic of Sec. 6, where a two-dimensional discretized electron distribution and a one-dimensional discretized ion distribution, with some two-dimensional effects included, are used. Finally, a short discussion of the results obtained is presented in Sec. 7.

It should be mentioned that the present paper represents a kind of a diary of our studies into ion-acoustic turbulence of fully-ionized plasmas. We feel that a unemotional tale of our calvary towards an at least partial answer could profit to others. Bad models should be known as much as promising ones.

2. BASIC EQUATIONS

We consider a uniform, collisionless, unmagnetized plasma consisting of hot electrons drifting with a constant velocity $\underline{V}_e = V_e \underline{e}_x$ relative to a cold ion background ($T_i << T_e$). The electron current generates ion-acoustic turbulence in the system, which results in anomalous resistivity. The constant current is sustained by an electric field $\underline{E} = E(t)\underline{e}_x$ varying in time in proportion to the resistivity.

../5

The problem stated here may be studied on the basis of simple quasilinear equations which include resonant and nonresonant wave-particle interactions. For a complete description nonlinear wave-particle-wave processes would have to be included as well. The aim of this paper is, however, to show that the nonresonant interaction of ions with waves is an important feature in ion-acoustic turbulence as anticipated by Dum et al.[8] For simplicity, we therefore neglect the nonlinear processes.

We will use throughout the paper the following dimensionless units:

$$t \to t/\omega_{pe},\ \underline{k} \to \underline{k}/\lambda_{deo},\ T_e \to T_{eo},$$

$$T_i \to T_i T_{eo},\ \underline{E} \to \frac{T_{eo}}{e\lambda_{deo}}\underline{E},\ \mathcal{E}_{\underline{k}} \to 4\pi n T_{eo}\lambda_{deo}^{p}\mathcal{E}_{\underline{k}}, \tag{1}$$

$$f^{(s)} \to \frac{n}{v_{the}^{p}} f^{(s)}$$

Here ω_{pe} is the electron plasma frequency, λ_{deo} the Debye length evaluated with the initial electron temperature T_{eo}, and $\mathcal{E}_{\underline{k}}$ is the spectral distribution associated with the ion-acoustic oscillations. The thermal velocity is given by $v_{theo}^{2} = T_{eo}/m_e$, where m_e is the electron mass. p = 1, 2 or 3 indicates the dimension of the velocity or the wavenumber (k-) space. $\mu_e = -1$ and $\mu = \mu_i = m_e/m_i$ are the dimensionless forms of e_s/m_s. With the above stipulations the equation describing the evolution of the spatially-averaged distribution function

../6

$f^{(s)}(\underline{v},t)$ for species s reads[19]

$$\frac{\partial f^{(s)}}{\partial t} = \frac{\partial}{\partial \underline{v}} \cdot \underline{\underline{D}}^{(s)} \cdot \frac{\partial f^{(s)}}{\partial \underline{v}} - \mu_s \underline{E} \cdot \frac{\partial f^{(s)}}{\partial \underline{v}} \tag{2}$$

where

$$\underline{\underline{D}}^{(s)} = \underline{\underline{R}}^{(s)} + \underline{\underline{S}}^{(s)} \tag{3}$$

The resonant part of the electron diffusion tensor $D^{(e)}$ is given by

$$\underline{\underline{R}}^{(e)} = 2\pi \int \frac{d^p k}{(2\pi)^p} \mathcal{E}_{\underline{k}} \frac{\underline{k}:\underline{k}}{k^2} \delta(\underline{k} \cdot \underline{v} - \omega_{\underline{k}}), \tag{4}$$

and the nonresonant or sloshing part by

$$\underline{\underline{S}}^{(e)} = 2 \int \frac{d^p k}{(2\pi)^p} \gamma_{\underline{k}} \mathcal{E}_{\underline{k}} \frac{\underline{k}:\underline{k}}{k^2} \mathcal{P} \frac{1}{(\underline{k}\cdot\underline{v}-\omega_{\underline{k}})^2}, \tag{5}$$

where the growth rate

$$\gamma_{\underline{k}} = \frac{\pi}{k^2 \frac{\partial \varepsilon}{\partial \omega}\Big/_{\omega_{\underline{k}}}} \int d^p v \; \underline{k} \cdot \frac{\partial F}{\partial \underline{v}} \; \delta(\omega_{\underline{k}} - \underline{k} \cdot \underline{v}). \tag{6}$$

The integrals in Eqs. (4) and (5) are restricted to $k_z > 0$. $F(v,t)$ is the combined distribution function, $F = f^{(e)} + \mu f^{(i)}$. The wave frequency $\omega_{\underline{k}}$ is given by $\varepsilon(\underline{k},\omega_{\underline{k}}) = 0$, where

$$\varepsilon(\underline{k},\omega_{\underline{k}}) = 1 - \frac{1}{k^2} \int d^p v \; \frac{\underline{k} \cdot \frac{\partial F}{\partial \underline{v}}}{\underline{k}\cdot\underline{v}-\omega_{\underline{k}}} \tag{7}$$

The ion diffusion tensors $\underline{\underline{D}}^{(i)}$, $\underline{\underline{R}}^{(i)}$, and $\underline{\underline{S}}^{(i)}$ are obtained by multiplying the corresponding electron tensors by μ^2 e.g. $\underline{\underline{D}}^{(i)} = \mu^2 \underline{\underline{D}}^{(e)}$.

../7

Finally, the evolution of the spectral distribution is described by

$$\frac{\partial \mathcal{E}_{\underline{k}}}{\partial t} = 2\gamma_{\underline{k}} \mathcal{E}_{\underline{k}} \, . \tag{8}$$

The Eqs. (2) - (8) will now be solved under several different assumptions in the following sections.

3. MAXWELLIAN PARTICLE DISTRIBUTION FUNCTIONS (moment approach)

The main assumption here is that the particle distribution functions maintain a Maxwellian shape in the course of time, i.e.

$$f^{(s)} = \frac{1}{(2\pi)^{\frac{1}{2}} v_{ths}} \exp\left[-\frac{1}{2} \frac{(v-V_s)^2}{V_{ths}^2} \right] , \tag{9}$$

where $v_{the}(t) = T_e^{\frac{1}{2}}$ and $v_{thi}(t) = (\mu T_i)^{\frac{1}{2}}$. We have assumed one-dimensionality, an assumption which does not qualitatively affect the results as long as we maintain Maxwellian distribution functions. The same remark holds for the additional assumptions which we want to make here, namely $\mu T_i << (\omega/k)^2 \lesssim V_e^2 << T_{eo}$ and $V_i = 0$. To lowest order therefore, we can write the real part of the usual dielectric response function

$$\varepsilon(k,\omega;t) = 1 - \mu/\omega^2 + \frac{1}{k^2 T_e(t)} \tag{10}$$

instead of Eq. (7).

Since our study is restricted to the case of an imposed constant current, V_e = const, the evolution of the particle distributions is fully described by the evolution of the temperatures. The pertinent equations may be derived from Eq. (2) by taking the second moment and

using the above-mentioned approximations[13]

$$\dot{T}_e = \frac{2}{\sqrt{2\pi}} \frac{V_e^2}{T_e^{3/2}} \int dk \frac{\mathcal{E}_k}{R} \left(1 - \frac{\phi_k}{V_e}\right)^2 + \frac{2}{\pi} \frac{1}{T_e} \int dk \frac{\gamma_k \mathcal{E}_k}{k^2} , \tag{11}$$

$$\dot{T}_i = \frac{2}{\sqrt{2\pi}} \frac{V_e^2}{T_e^{3/2}} \int dk \frac{\mathcal{E}_k}{k} \left(1 - \frac{\phi_k}{V_e}\right) \frac{\phi_k}{V_e} - \frac{2\Lambda}{\pi} \int dk \gamma_k \mathcal{E}_k \left(1 + \frac{1}{k^2 T_e}\right). \tag{12}$$

The dot denotes time derivatives and $\phi_k = \omega_k/k$ is the phase velocity of the waves. The first term in Eq. (11) stems from the resonant interaction, Eq. (4), the second term from the nonresonant interaction, Eq. (5). With $\Lambda = 1$, Eq. (12) gives $\dot{T}_i$ due to both resonant and nonresonant interactions. The effect of resonant interaction can be singled out by choosing $\Lambda = 2$.

For a numerical treatment of Eq. (11) and (12) together with Eq. (8) a discrete spectral distribution $\mathcal{E}_k$ is needed. In the context of the present section one could just opt for the usual equally spaced discrete waves.[13,18] Instead of this, however, we introduce a finite element approximation as it will be required in subsequent sections for convergence reasons, i.e.:

$$\mathcal{E}_k(t) = \sum_{\ell=1}^{L} \mathcal{E}_\ell(t)\, \chi_\ell(k). \tag{13}$$

The piecewise constant basis functions $\chi_\ell(k)$ are defined by

$$\chi_\ell(k) = \begin{cases} 1 & k_\ell \leq k \leq k_{\ell+1} \\ 0 & \text{elsewhere} \end{cases} , \tag{14}$$

../9

assuming some discrete k-mesh $k_1 < k_2 < \ldots\ldots < k_{L+1}$. The discrete form of Eq. (8) then reads

$$\dot{\mathcal{E}}_\ell = \Gamma_\ell \, \mathcal{E}_\ell \qquad \ell = 1, \ldots\ldots, L \tag{15}$$

where

$$\Gamma_\ell = \frac{2}{k_{\ell+1} - k_\ell} \int_{k_\ell}^{k_{\ell+1}} dk \;\; \gamma_k \quad . \tag{16}$$

The Eqs. (11), (12) and (15) are now solved numerically, stepping in time by means of a simple time centered finite difference scheme.[18] The k-integrals from k_ℓ to $k_{\ell+1}$ are evaluated numerically by Simpson's rule.

In Fig. 1 the temporal evolution of the electrostatic fluctuation energy

$$W = \tfrac{1}{2} \int \frac{d^p k}{(2\pi)^p} \; \mathcal{E}_{\underline{k}} \tag{17}$$

is shown together with the evolution of the ion temperature, T_i. The qualitative behaviour of these quantities is quite insensitive to whether only the resonant interaction ($\Lambda = 2$ in Eq. (12)) or both the resonant and nonresonant interactions are active. Moreover, the qualitative behaviour does not depend on the initial conditions as long as $W(t=0)$ and $T_i(t=0)$ are sufficiently low. The quantitative behaviour, however, must evidently depend on the model chosen as well as on the initial parame-

../10

ters. The evolution in Fig. 1 has been obtained with $V_e = 0.12$, $T_{eo} = 1$, $T_{io} = 0.01$, $W(0) = 2.7 \times 10^{-5}$, $\mu = 1/1836$ and 15 waves, equally spaced between $k_1 = 0.05$ and $k_{16} = 1.55$.

The most important feature of the evolution is the fact that the instability is quenched. The mechanism is easy to understand. The Maxwellian shape of the ion distribution function being maintained during the evolution, the ion Landau damping increases rapidly with increasing ion temperature and eventually overcomes the electron growth rate. This saturation, however, is entirely unphysical in the case where the ions merely interact resonantly with the waves. In our model the resonant interaction affects the whole ion distribution function thus increasing the number of resonant particles. The slope of the distribution function in the resonant region being imposed by the Maxwellian shape, the ion Landau damping must increase accordingly. In reality the resonant interaction operates locally in velocity space; no bulk heating and no increase of resonant ions can result, and the ion Landau damping will always tend to decrease under the influence of mere resonant interaction. The inclusion of nonresonant interaction, which provides physical means for particle exchange between the resonant and the nonresonant region, does not render our model much more reliable.

It appears that evolving global distribution functions are of limited utility in problems where the wave-particle interaction is the dominant part of the physics involved. They might, however, permit reasonable estimations concerning turbulent phenomena in strongly collisional plasmas.

../11

4. DISCRETE PARTICLE DISTRIBUTION FUNCTIONS

4.1 Discrete 1D ion distribution function

We now turn our attention to the local evolution of the ion distribution function $f^{(i)}(v,t)$, in velocity space. One might argue that a one-dimensional model should be sufficient, since the formation of a tail extending primarily in the direction of the electron drift is expected. This model will at least enable us to study consistently the transfer by nonresonant interaction, of bulk ions into the resonant region.

For the sake of simplicity we use as a first approximation a one-dimensional wave spectrum. As a consequence we have to maintain a Maxwellian electron distribution function in order to prevent immediate saturation due to the formation of a plateau.[15] This is a purely one-dimensional effect, which has been treated in detail elsewhere[17] and is not of interest here.

We now derive a discrete form of the one-dimensional ion kinetic equation, (Eq. (2), that allows for local response. Firstly, Eq. (2) is put into the weak form[20] imposing natural (Neumann) boundary conditions on the distribution function. The convection term due to the electric field E_x, can be removed by a transformation into the frame of freely accelerated ions. The corresponding term in the electron equation may then be considered negligible. The only effect of this approximation is that the overall momentum conservation is violated. The next

../12

step is to approximate the distribution function by a finite element expansion,

$$f^{(i)}(v,t) = \sum_{m=1}^{M+1} f_m^{(i)}(t)\ \psi_m(v). \tag{18}$$

In equations concerning the ions v will always be used to denote v_x. The basis functions $\psi_m(v)$, are the standard roof functions,

$$\psi_m(v) = \begin{cases} 0 & v \leq v_{m-1} \\ \dfrac{v-v_{m-1}}{v_m-v_{m-1}} & v_{m-1} \leq v \leq v_m \\ \dfrac{v_{m+1}-v}{v_{m+1}-v_m} & v_m \leq v \leq v_{m+1} \\ 0 & v_{m+1} \leq v \end{cases} \tag{19}$$

corresponding to the simplest choice possible for second order differential equations. A discrete v-mesh, $v_1 < v_2 < \cdots\cdots\cdots < v_{M+1}$ is assumed.

Making use of the expansion, Eq. (18), we obtain the discrete version of Eq. (2)

$$A_{mn}^{(i)}\ \dot{f}_n^{(i)} = (R_{mn}^{(i)} + S_{mn}^{(i)})\ f_n^{(i)} \qquad m = 1, \ldots\ldots, M+1 \tag{20}$$

where the sum symbol over repeated indices has by convention been omitted.

../13

Further

$$A_{mn}^{(i)} = \int \psi_m \psi_n \, dv \tag{21}$$

is the mass matrix,

$$R_{mn}^{(i)} = - \mu^3 \mathcal{E}_\ell \int dv \, \frac{\chi_\ell(k_v)}{k_v^2 v^3} \psi_m' \psi_m' \tag{22}$$

the resonant interaction matrix and

$$S_{mn}^{(i)} = - \frac{\mu^3}{\pi} \mathcal{E}_\ell \int dv \, \psi_m' \psi_n' \int dk \, \frac{\gamma_k \chi_\ell(k)}{k^3 \phi_k^3} \, \frac{\mathcal{P}}{(v-\phi_k)^2} \tag{23}$$

the nonresonant interaction matrix. The primes denote derivations with respect to v. The spectral density has been inserted in its finite element form, Eq. (13). The wavenumber k_v in Eq. (22) is a function of v and t according to the simplified dispersion relation, Eq. (10), $k_v^2 = \mu/(v-V_i)^2 - 1/T_e$, where we have retained the quasilinearly produced ion drift V_i. On the other hand, in Eq. (23) the phase velocity ϕ_k depends upon k and t, $(\phi-V_i)^2 = \mu/(k^2 - T_e^{-1})$. The integrals in Eqs. (22) and (23) are numerically evaluated using a three-point Simpson's rule per interval. The principal value is approximated by

$$\mathcal{P} \frac{1}{x^2} = (x^2 - \delta^2) \, / \, (x^2 + \delta^2)^2. \tag{24}$$

The width δ is to be taken of the order of the velocity mesh size in the resonant region, i.e. in the region where $x = v - \phi_k = 0$.

../14

The Eqs. (11), (15) and (22) form a complete set of ordinary differential equations in time. In order to show clearly the effects due to the local response of the ion distribution function in the resonant region we supplement these equations with the same initial conditions as in the previous section. The result, indicated by open circles, is presented in Fig. 2. For easy comparison the result obtained in the previous section with $\Lambda = 1$ is shown again (continued line). First of all, we observe that the fluctuation energy does not saturate although the ion temperature keeps increasing with time. The reason for this behaviour can be found from an inspection of the quantity $\langle \gamma_i/\gamma_e \rangle$ which is the ratio of the ion damping rate to the electron growth rate averaged over the wave amplitudes. The nonresonant interaction steadily brings new bulk particles into the resonant region where in principle they could establish and maintain a strong negative slope and hence induce strong ion Landau damping. The fact that the ratio $\langle \gamma_i/\gamma_e \rangle$ always remains much smaller than one, however, indicates that the resonant interaction is strong enough to maintain a sort of plateau in spite of the ion influx from the bulk. This behaviour is further illustrated by Fig. 3, where the ion distribution function together with the fluctuation spectrum is shown at a time near to the saturation point of the previous model, $t = 5000$.

We have performed many runs with different initial conditions, different drift velocities and different mass ratios μ. In none of these runs we have found saturation. The absolute value of $\langle \gamma_i/\gamma_e \rangle$ was never bigger than about 0.5. All the runs ended with a "pathological" ion distribution: $f^{(i)}(v=0)$ was decreasing in time due to the reversible nonresonant

../15

heating and due to the particle transfer to the resonant region until it was as small as the growing plateau. This situation occurred at fluctuation energies of the order of 0.05 to 0.1. Generally we accepted the results as long as the tail did not comprise more than one third of the ions.

4.2 Discrete ion and electron distributions

Before we discuss the tail formation in detail in the next section, we first turn our attention to the local quasilinear modification of the electron distribution function. We hope that the quasilinear depression of the electron growth rate suffices to bring the ratio $\langle \gamma_i/\gamma_e \rangle$ above unity and that saturation of the wave energy results. As mentionned earlier the quasilinear treatment of the electrons must be more than one-dimensional. The reason is that in most cases the turbulent ion-acoustic waves have a broad angular distribution and interact with almost all electrons resonantly. The simplest model which takes this fact into account and which does not prevent electron run-away is two-dimensional. Ideally we would therefore like to solve Eqs.(2) and (8) in two dimensions. Unfortunately the structure of the nonresonant interaction term, (Eq. (5), is rather formidable: each particle interacts with each wave, or expressed in terms of a numerical method, it means that each velocity cell interacts with each wavenumber cell. This prohibits us from searching for a numerical solution of Eqs. (2) and (8) as they stand.

../16

In order to find possible simplifications we note first, that the ways in which the electron and the ion populations interact with the waves differ distinctly. Almost all electrons undergo resonant and nonresonant interactions, whereas only the tail ions are resonant. The electron distribution function is modified globally by both processes which act somehow independantly of each other. Their relative importance may be estimated from the two terms in Eq. (11) yielding

$$\frac{(\dot{T}_e)_{NR}}{(\dot{T}_e)_R} \approx \frac{\mu^{\frac{1}{2}} T_e^{\frac{1}{2}}}{2V_e} \quad . \tag{25}$$

For most cases of interest this quantity is much smaller than one and we therefore neglect the nonresonant term in the electron equation. As we have already learned we may not do so in the ion equation. Hence the only way to simplify the ion part is to make it one-dimensional. This may be achieved by assuming the distribution function to be narrow in the direction perpendicular to the driving current, i.e. $f^{(i)}(v_x,v_y,t) = f^{(i)}(v_x,t)\ \delta(v_y)$. Integration of Eq. (2) over v_y then yields

$$\frac{\partial f^{(i)}(v,t)}{\partial t} = -\frac{\partial}{\partial v}\left(R^{(i)} + S^{(i)}\right)\frac{\partial f^{(i)}}{\partial v} \tag{26}$$

where the electric field term has been dropped. Again v stands for v_x.

../17

The diffusion coefficients are simply

$$R^{(i)} = 2\pi\mu^2 \int \frac{d^2k}{(2\pi)^2} \quad \mathcal{E}_{\underline{k}} \frac{k_x^2}{k^2} \delta\,(k_x v - \omega_{\underline{k}}), \tag{27}$$

$$S^{(i)} = 2\mu^2 \int \frac{d^2k}{(2\pi)^2} \gamma_{\underline{k}} \mathcal{E}_{\underline{k}} \frac{k_x^2}{k^2} \mathcal{P} \frac{1}{(k_x v - \omega_{\underline{k}})^2} \quad . \tag{28}$$

The growth rate $\gamma_{\underline{k}}$ Eq. (6), follows directly from $f^{(i)} \propto \delta(v_y)$. The dielectric function Eq. (7), is evaluated consistently with the same 1D ion distribution. Retaining the electron and ion drifts to lowest order we find

$$k^2 \left.\frac{\partial \varepsilon}{\partial \omega}\right|_{\omega_{\underline{k}}} = 2 \left(\frac{\mu k_x^2}{(\omega_{\underline{k}} - k_x V_i)^3} + \frac{k_x V_e}{k^2 T_e^2} \right) \tag{29}$$

and

$$(\omega_{\underline{k}} - k_x V_i)^2 = \frac{\mu T_e k_x^2}{1 + k^2 T_e - k_x^2 V_e^2/(k^2 T_e)} \quad . \tag{30}$$

We now have a complete set of differential equations: Eq. (2) for the electrons where $\underline{\underline{D}}^{(e)}$ is replaced by $\underline{\underline{R}}^{(e)}$, Eq. (26) for the ions and Eq. (8) for the fluctuations. The set is supplemented by the relations given in Eqs. (4), (6) and (27) through (30). With respect to the discretization it is evident that the most difficult is the resonant interaction between waves and electrons, since both populations are two-dimensional. A few years ago we described a method which allows us to tackle this problem[18] and applied it to Langmuir turbulence. It

../18

is trivial to adapt from Langmuir to ion-acoustic turbulence; only the relations concerning wave dispersion, i.e. the relations for $\partial\varepsilon/\partial\omega$ and for $\omega_{\underline{k}}$, Eqs. (29) and (30), have to be changed. Moreover, in the ion-acoustic problem these quantities depend upon time through $V_e(t)$ and $T_e(t)$ and need a frequent up-dating.

In [18] the discretization of the electrons is achieved with pyramidal basis functions $\Psi_m(V_x,V_y)$ upon a rectangular mesh subdivided into triangles. The waves have been represented by equally-spaced single points in k-space. We found later that the waves should be expanded in finite elements for technical reasons: the number of input-output operations from core to disc and back may be cut down by a fair factor in this way. We give therefore a short description of how the wave spectrum may be approximated by finite elements. The procedure is analogue to the one used in Eqs. (13) and (14). The finite rectangular k-space is subdivided into small rectangles ρ_ℓ with area $(\Delta^2 k)_\ell$ of irregular size. The basis function $\chi_\ell(k_x,k_y)$ takes the value one on the small rectangle ρ_ℓ and is zero elsewhere. Integrals over small rectangles ρ_ℓ are performed numerically using J = 4, 9 or 16 integration points $\underline{k}_\ell^j$ with equal weight according to the precision needed for good convergence. Each of these integration points may be viewed as one "single-point-wave" as used in [18]. Then the discretized forms of the electron equations follow directly from there. The kinetic equation, Eq. (2), becomes

$$A_{mn}^{(e)}\dot{f}_n^{(e)} = (R_{mn}^{(e)} + EC_{mn})\, f_n^{(e)}, \tag{31}$$

../19

where the mass matrix

$$A_{mn}^{(e)} = \int \Psi_m \Psi_n \, d^2v \quad , \tag{32}$$

the resonant interaction matrix

$$R_{mn}^{(e)} = -2\pi \sum_{\ell} \frac{\mathcal{E}_{\ell} (\Delta^2 k)_{\ell}}{(2\pi)^2} \frac{1}{J} \sum_{j=1}^{J} \left[\frac{1}{k^2} \int_{\tau_{\underline{k}}} ds \left(\underline{k} \cdot \frac{\partial \Psi_m}{\partial \underline{v}}\right) \left(\underline{k} \cdot \frac{\partial \Psi_n}{\partial \underline{v}}\right) \right]_{\underline{k} = \underline{k}_{\ell}^{j}} , \tag{33}$$

and the electric field matrix

$$C_{mn} = \int \Psi_m \frac{\partial \Psi_n}{\partial v_x} \, d^2v \, . \tag{34}$$

The quantity ds in Eq. (33) denotes a line element in velocity space and the straight line $\tau_{\underline{k}}$ is defined by

$$\underline{k} \cdot \underline{v} - \omega_{\underline{k}} = 0 \, . \tag{35}$$

If we approximate the total growth rate by

$$\Gamma_{\ell} = \frac{2}{(\Delta^2 k)_{\ell}} \int_{D_{\ell}} \gamma_{\underline{k}} d^2k = \Gamma_{\ell}^{(e)} + \Gamma_{\ell}^{(i)} \tag{36}$$

../20

we can immediately write down the electron part, namely

$$\Gamma_{\ell}^{(e)} = \sum_{m=1}^{n} f_m^{(e)} \frac{1}{J} \sum_{j=1}^{J} \left[\frac{2\pi}{k^2 \frac{\partial \varepsilon}{\partial \omega}\Big|_{\omega_{\underline{k}}}} \int_{\tau_{\underline{k}}} ds\, \underline{k} \cdot \frac{\partial \Psi_m}{\partial \underline{v}} \right]_{\underline{k} = \underline{k}_{\ell}^{j}} . \qquad (37)$$

There remains one difficulty: we do not want to impose the field E but rather the current V_e. E is determined by the anomalous resistivity. One can obtain an expression for E directly from Eq. (31) using the relation

$$\dot{V}_e = \int v_x \dot{f} d^2v = (v_x)_m A_{mn} \dot{f}_n^{(e)} = 0. \qquad (38)$$

Hence

$$E = - \frac{(v_x)_m R_{mn}^{(e)} f_n^{(e)}}{(v_x)_m C_{mn} f_n^{(e)}} \qquad (39)$$

at each instant. In the code the nonlinearity brought in by Eq. (39) is treated in a time explicit manner which ensures that an eventual small deviation of the actual drift velocity $(v_x)_m A_{mn} f_n^{(e)}$ from the imposed value V_e disappears within one time step :

$$E(t + \frac{\Delta t}{2}) = - \frac{(v_x)_m R_{mn}^{(e)} f_n^{(e)} + \frac{1}{\Delta t} \left[(v_x)_m A_{mn} f_n^{(e)} - V_e \right]}{(v_x)_m C_{mn} f_n^{(e)}} . \qquad (40)$$

The discretization of the ion equation, Eq. (26), is done as previously, Eqs. (18) through (24). The form of the kinetic equation,

../21

Eq. (20), remains the same, only the expressions for the interaction matrices, derived from Eqs. (27) and (28) differ :

$$R_{mn}^{(i)} = -\mu^2 \sum_{\ell=1}^{L} \frac{\mathcal{E}_\ell (\Delta k_y)_\ell}{2\pi} \int_{(\Delta k_x)_\ell} dk_x \frac{k_x}{k_x^2+(k_y)_\ell^2} \left[\psi'_m \psi'_n \right] v = \omega_{\underline{k}}/k_x \quad , \tag{41}$$

$$S_{mn}^{(i)} = -\frac{\mu^2}{\pi} \sum_{\ell=1}^{L} \frac{\Gamma_\ell \mathcal{E}_\ell (\Delta k_y)_\ell}{4\pi} \int_{(\Delta k_x)_\ell} dk_x \frac{1}{k_x^2+(k_y)_\ell^2} \int dv \, \psi'_m \psi'_n \frac{\mathcal{P}}{(v-\phi_{\underline{k}})^2} \, . \tag{42}$$

The growth rate is given by

$$\Gamma_\ell^{(i)} = \frac{2}{(\Delta k_x)_\ell} \int_{(\Delta k_x)_\ell} dk_x \left[\frac{\mu\pi}{k^2 \frac{\partial \varepsilon}{\partial \omega}\Big|_{\omega_{\underline{k}}}} f_n^{(i)} \psi'_n \left(\frac{\omega_{\underline{k}}}{k_x}\right) \right]_{\underline{k} = \left[k_x, (k_y)_\ell \right]} \, . \tag{43}$$

The Eqs. (15), (20) and (31) can now be solved in time using the relations (21), (29), (30), (32) through (37) and (40) through (43). In Fig. 4 the temporal evolution of the electrostatic fluctuation energy W, Eq. (17), is shown together with the ratio $\langle \gamma_i/\gamma_e \rangle$. The initial conditions for this run are $V_e = 0.12$, $T_{eo} = 1$, $T_{io} = 0.02$, $\mu = 1/1836$ and $W(0) = 4\times10^{-10}$. The ions are described within the interval $v = [-0.03, 0.1]$ which is subdivided by 38 nonequidistant points. The electron distribution is given on a quadratic domain, $v_x = [-8., +8.]$ and $v_y = [-8., +8.]$ which is subdivided into small rectangles of irregular size by 23 lines with v_x = const and 18 lines with v_y = const

../22

resulting in M = 500 grid points. As far as the waves were concerned, we used a domain given by $k_x = [0., 2.]$ and $k_y = [-2., +2.]$, which is subdivided by 8 lines with k_x = const and 10 lines with k_y = const resulting in L = 99 waves.

All the runs we made with different initial conditions and different discretization parameters have shown qualitatively the same behaviour as the one presented in Fig. 4. We never found saturation. The wave energy always increased at a slower and slower rate but we never observed a $\langle\gamma_i/\gamma_e\rangle$ larger than one. However, we did not push these calculations to their extreme limits in time, because after a set of runs of this kind we were convinced that the multi-dimensionality would be important even in the ion dynamics.

It was not just the run shown in Fig. 4 that led to this conclusion. We had also made numerical experiments where we imposed artificial electron growth rates $\gamma_e(t)$ with ad hoc chosen different time dependancies. We found that the qualitative behaviour of W and $\langle\gamma_i/\gamma_e\rangle$ was once more the same as in Fig. 4. Only the time scale was influenced by $\gamma_e(t)$. The conclusion was that our sophisticated 2D-2D-1D-model could not produce results qualitatively different from those in Sec. 4.1.

../23

5. ION TAIL FORMATION BY NONRESONANT WAVE-PARTICLE INTERACTION

The results of the numerical experiments with imposed $\gamma_e(t)$ show that the 2D-2D-1D-model is not significantly better than the simple model of Sec. 4.1 where the electron distribution function is represented by a Maxwellian. This latter can certainly not give correct time scales, because the γ_e will always be overestimated due to the absence of the quasilinear flattening; but it can be used to study the ion tail formation by nonresonant interactions which, apart from the time scale, appear to be independent of γ_e.

Firstly, we demonstrate that the ion tail formation is indeed not inconsistent with the observations made in particle simulations[8]. In Fig. 5 the evolution of the wave energy is shown together with the temperatures and the number of ions in the tail,

$$n_t = \int_{v_o(t)}^{\infty} f^{(i)} dv \quad , \tag{44}$$

where v_o is given by the phase velocity of the slowest initially unstable ion-acoustic wave. n_t is therefore the number of resonant particles. The initial conditions are $V_e = 0.75$, $T_{eo} = 1$, $T_{io} = 0.01$, $\mu = 1/100$ and $W(0) = 1.3 \times 10^{-6}$. At t=250 the values of the plotted parameters approximately coincide with those of the particle simulation[8] at t=0. At t=500 the fluctuation energy has reached the value 0.039 corresponding to the saturation value in the particle simulation. From

../24

the fact that the saturation occurs at t=700 we deduce that our time scales, as expected, are too small. The discrepancy is roughly a factor 3. Let us compare now the other quantities at equal W, W=0.039. We find $T_e = 4$, $T_i/T_e = .15$, $n_t = 0.3$, whereas the particle simulation results are $T_e = 3.8$, $T_i/T_e = .10$, $n_t = 0.2$ (?). These quantities compare favourably. We question the value of n_t because the method of estimation used in the particle simulation case may be different to that used here, Eq. (44); also in the paper[8] n_t is given for the final time, t=1000. It seems, however, that our model overestimates the number of hot ions. Nevertheless one can say that the agreement is remarkably good and that there is no doubt about the importance of the nonresonant wave-particle interaction for the formation of high energy ions.

Next, we investigate the relation between W and n_t for different initial conditions. Since time is meaningless in this model, it is removed by plotting $n_t(t)$ versus W(t) during the evolution. First of all, we find that the curve $n_t(W)$ depends on neither μ nor V_e which is the result that was expected from the runs with imposed γ_e. For this to be possible, the average γ_i must always be substantially smaller than the average γ_e, otherwise γ_i would influence the ion tail formation through the nonresonant diffusion term, Eq. (5), $S^{(i)} \propto \gamma_e + \gamma_i$. The only parameters which can influence the behaviour of $n_t(W)$ are $n_t(t=0)$ and W(t=0) themselves. In Fig. 6 the behaviour for three different initial fluctuation levels is shown. All three curves converge for increasing energy. This once more tells us simply that the dynamics of γ_i has no direct influence on the production of hot ions. In runs with different initial

../25

temperatures, hence different initial n_t, one sees the same phenomenon: at energies of the order of 0.02 one finds roughly 20% of the particles in the tail as in Fig. 6. It is noteworthy that the mean wavevector <k> of the fluctuations at W = 0.02 depends upon the initial temperature T_{io}. For the values T_{io} = 0.01 and 0.03 we found <k> = 1.2 and 0.7 respectively. Since $S^{(i)}$ has a $1/k^2$ dependance, Eq. (5), one would expect the tail production to depend upon <k>. That this is not the case indicates that the tail production results from a subtle interplay between the resonant and the nonresonant interactions.

A further comment on Figs. 5 and 6 is that as soon as we initialize the fluctuation level to a value above 2×10^{-4}, saturation occurs at an energy barely 10% higher than the initial level. The first sign of this phenomenon can already be seen in the case $W(0) = 5\times10^{-5}$ in Fig. 6, where the curve strangely bends back. It is evident that under these circumstances our weak turbulence model fails due to the neglect of discrete particle effects (i.e. spontaneous emission and related friction). It was for this reason that the initial condition of the particle simulation, W(0) = .005, could not be used to produce Fig. 5.

From this section we retain that the nonresonant wave-particle interaction produces substantial fractions of resonant particles consistent with observations. However, as we have already seen in Sec. 4.1 their distribution remains too flat and does not induce strong Landau damping.

../26

6. SATURATION AS A MULTI-DIMENSIONAL QUASILINEAR EFFECT

In the model with a 1D ion distribution the resonant particles are confined to a domain in v-space which is bounded from above by $v = \max(\omega_k/k) = c_s = (\mu T_e)^{\frac{1}{2}}$, the ion-sound velocity. Such an upper bound does not exist in a multi-dimensional situation, because the relation to be satisfied by a resonant particle is merely $\underline{v} \cdot \underline{k} = \omega_{\underline{k}}$. This means that a particle with $|\underline{v}| > c_s$ can interact with all waves having a $\underline{k}$ such that $\underline{v} \cdot \underline{k} = \omega_{\underline{k}}$. Hence we may hope that the resonant wave-particle interaction speeds particles up to velocities higher than c_s. Ion tails extending up to 2 c_s have indeed been seen in particle simulations[8]. In turn, we can hope that the ion distribution in this extended resonant region remains steeper than in the 1D case, offering therefore the possibility of saturation.

In order to test these ideas we incorporate the effect of more dimensions in the model presented in Sec. 4.2. As mentioned there, due to the complexity of the nonresonant term, we cannot permit ourselves to treat the ions really in more dimensions. The multi-dimensionality, however, seems to be crucially important only for the resonant interaction. We replace therefore the 1D Dirac delta-functions in $R^{(i)}$, Eq. (4), and in $\gamma^{(i)}$, Eq. (6), by a broadened resonance function, which takes the multi-dimensionality into account. A reasonable form of this function may be found by assuming for a while that the ions are isotropic in two dimensions. Going back then by brute force

../27

to 1D we find that $\delta(v-\omega_{\underline{k}}/k)$ has to be replaced by the function

$$G(k,v) = \begin{cases} \frac{2}{\pi} \frac{\omega_{\underline{k}}}{vk_x} (v^2 - \omega_{\underline{k}}{}^2/k_x{}^2)^{-\frac{1}{2}} & v > \omega_{\underline{k}}/k_x \\ 0 & v < \omega_{\underline{k}}/k_x \end{cases} , \tag{45}$$

which has the same norm as the δ-function. The introduction of this new resonance function into $R^{(i)}$ and $\gamma^{(i)}$, Eqs. (4) and (6) respectively, and the subsequent discretization are straightforward. The nonresonant interaction term, Eq. (42), is divided by 2, thus accounting for the two degrees of freedom in which the distribution function is affected by the nonresonant heating.

Using this new model we have finally found saturation, Fig. 7. The initial conditions for this run are similar to those in Sec. 3 and 4: $V_e = 0.12$, $T_{eo} = 1$, $T_{io} = 0.02$, $W(0) = 4 \times 10^{-10}$ and $\mu = 1/1836$. The velocity and wavevector meshes are the same as for Fig. 4. We do not believe that too much importance should be attached to the quantitative result, $W_{sat} = 0.01$ and $-E_{max} = 5.7 \times 10^{-5}$, bearing in mind that we have made a rather crude approximation to the real 2D situation. The same remark obviously holds for other quantities such as T_e, T_i, and the explicit shapes of $f^{(e)}$, $f^{(i)}$ and $\mathcal{E}_{\underline{k}}$. Since we have completely documented the general behaviour of these quantities elsewhere[21] for

../28

a run with $V_e = 0.75$, $T_{io} = 0.02$ and $\mu = 1/100$, we restrict our interest here to the tail formation. Fig. 8 shows the evolution of the ion distribution function in the tail region for the run shown in Fig. 7. Up to the saturation time, $t = 1.1 \times 10^5$, the number of particles in the tail increases steadily and the tail extends roughly up to $2c_s(t)$. At saturation the particle influx from the bulk ceases leaving the number of resonant particles unchanged in the further evolution, whereas their energy still increases due to the resonant interaction. At the final time, $t = 3.6 \times 10^5$, the tail extends to almost $3c_s$. The number of tail particles at saturation is 1.5%. This figure is roughly one order smaller than what we expect from our 1D calculations, Fig. 6. There are several reasons for this. First of all we have divided the nonresonant interaction term by a factor 2 in order to simulate a 2D ion distribution as mentioned above. A further factor 2 stems from the 2D waves because for equal energy increase, $\dot{W}$, the 2D nonresonant term is weighted by a factor $\langle k_x^2/k^2 \rangle \approx 0.5$ as compared to the corresponding 1D term. The remaining factor 2 may come from the fact that the resonant interaction near to the bulk is weaker than in the 1D case and is therefore less effective in evacuating particles brought in by the nonresonant interaction.

Runs with higher saturation energy showed substantially higher numbers of hot ions. For a saturation energy of 0.06, for example, we found 20% of hot ions. Even this number is markedly below the value obtained with the 1D model. A comparison with the values obtained

../29

in the simulations[8] indicates that the 2D model, although somewhat inconsistent, describes the ion tail formation better than the 1D model. Moreover, the number of hot ions produced with the 2D model depends slightly upon the electron to ion mass ratio: with higher ion masses we obtain at equal fluctuation energies less hot ions. This tendency has also been seen in the simulations. On the other hand no dependance upon the current V_e, has been observed.

There remain two important topics to be discussed: the nonresonant interaction for damped waves and nonlinear wave-wave-particle effects. As far as the nonresonant interaction is concerned, ten years ago there was some discussion about the sense or the nonsense of the so-called "negative diffusion" in quasilinear theory.[22,23] The nonresonant diffusion coefficient, $S^{(i)}$, may locally become negative whenever some growth rates become negative. In the nonresonant region where $R^{(i)} = 0$ the total diffusion coefficient is therefore negative, which is obviously a disaster. Starting from round-off and discretization errors the numerical solution will immediately blow up. A diffusion equation with negative coefficient describing a physical phenomenon is an absurdity and must stem from an erroneous handling of mathematical tools. In the case in question $S^{(i)}$ is locally of higher order than $R^{(i)}$ in an expansion in γ/ω. The importance of $S^{(i)}$ resides in its much larger support in velocity space; the influence of $R^{(i)}$ and $S^{(i)}$ is comparable only under the integral $\int dv$. $S^{(i)}$ should therefore only influence the global properties of the distribution function. Numerically we solve this problem in a pragmatic way. Whenever $R^{(i)} + S^{(i)}$ becomes negative in a specific velocity interval we

../30

replace $\partial/\partial v S^{(i)} \partial f^{(i)}/\partial v$ in this interval by $\partial/\partial v S^{(i)} \partial f_M^{(i)}/\partial v$; $f_M^{(i)}(v)$ is taken as the Maxwellian having the same momentum and energy as $f^{(i)}$. By means of this the negative diffusion term is replaced by a source term depending nonlinearly on integral quantities of $f^{(i)}$.

With respect to nonlinear wave-wave-particle effects, we believe that they are not negligible. We find that even resonance broadening could quantitatively affect our results in Fig. 7. The broadening evaluated for the spectrum corresponding to Fig. 7 turns out to be $\Delta(\omega_k/k) \approx c_s/2$. This value is at the extreme upper limit for the validitiy of the theory of resonance broadening. One could anticipate, however, that the inclusion of induced scattering in our model would not allow the fluctuation energy to grow to values where resonance broadening would be important.

7. CONCLUSIONS

We have used different one- and two-dimensional quasilinear models to study the evolution of current-driven ion-acoustic turbulence. We are not able to give definite quantitative answers because on the one hand, we have not considered nonlinear wave-wave-particle interactions and on the other hand, because we have treated the effects of the multidimensionality on the evolution of the ion distribution function in an approximate manner only. We did produce however strong evidence that

../31

the nonresonant wave-particle interaction is indeed responsible for the appearance of high energy ions during the evolution of ion-acoustic turbulence. We also have shown that these ions may quench the instability by linear Landau damping. As a by-product, we have found that models which use global particle distribution functions are of rather limited applicability in problems dominated by quasilinear effects.

Ion-acoustic turbulence seems to be a very difficult problem in the sense that a quantitative answer can only be hoped for in a complete multi-dimensional model including resonant and nonresonant wave-particle interactions and induced scattering.

../32

ACKNOWLEDGEMENTS

The authors acknowledge Professor E.S. Weibel for fruitful discussions. They also would like to thank Dr. A.D. Cheetham who carefully read and criticized the manuscript.

This work was supported by the Swiss National Science Foundation.

../33

REFERENCES

1. Y. Amagishi, A. Hirose, H.W. Piekaar, and H.M. Skarsgard, in Plasma Physics and Controlled Nuclear Fusion Research 1976 (International Atomic Energy Agency, Vienna, 1977) Vol. III, p. 11.

2. H. de Kluiver, C.J. Barth, H.J.B.M. Brocken, J.J.L. Caarls, B. de Groot, H.W. Kalfsbeek, H.W. Piekaar, A. Ravenstein, W.R. Rutgers, B. de Stigter, H.W.H. Van Andel, and H.S. Van der Ven in Plasma Physics and Controlled Nuclear Fusion Research 1978 (International Atomic Energy Agency, Vienna, 1979) Vol. II, p. 639.

3. J. Benford, V. Bailey, T.S.T. Young, D. Dakin, B. Ecker, S. Putnam, M. Di Capua, R. Cooper, D.A. Hammer, K. Gerber, K.R. Chu, R. Clark, M. Greenspan, J. Sethian, C. Ekdahl, C. Wharton, and L. Thode in Ref. 1, Vol. II, p. 543.

4. A.K.L. Dymoke-Bradshaw, A.E. Dangor, and J.D. Kilkenny, in Ref. 1, Vol II, p. 555.

5. R.C. Malone, R.L. McCrory, and R.L. Morse, Phys. Rev. Lett. 34, 721 (1975).

6. S.A. Kaplan and V.N. Tsytovich, Plasma Astrophysics (Pergamon, Oxford, 1973).

../34

7. E.K. Zavoiskii, B.A. Demidov, Yu.G. Kalinin, A.G. Plakhov, L.I. Rudakov, V.C. Rusanov, V.A. Skoryupin, G.E. Smolkin, A.V. Titov, S.D. Fanchenko, V.V. Shapkin, and G.V. Sholin, in Plasma Physics and Controlled Nuclear Fusion Research 1971 (International Atomic Energy Agency, Vienna, 1971) Vol. II, p.3.

8. C.T. Dum, R. Chodura, and D. Biskamp, Phys. Rev. Lett. 32, 1231 (1974).

9. J. Orens, Ph.D. Thesis, Princeton University (1974).

10. G.E. Vekshtein and R.Z. Sagdeev, Pis'ma v Zh. Eksp. Teor. Fiz. II, 297 (1970) {JETP Lett. II, 194 (1970)}.

11. W.M. Manheimer and R.W. Flynn, Phys. Fluids 17, 409 (1974).

12. R.L. Stenzel, Phys. Fluids 21, 99 (1978).

13. M.Z. Caponi and R.C. Davidson, Phys. Rev. Lett. 31, 86 (1973).

14. M.Z. Caponi and R.C. Davidson, Phys. Fluids 17, 1394 (1975).

15. Duk-in Choi and W. Horton Jr., Phys. Fluids 18, 858 (1975).

16. A.A. Vedenov, E.P. Velikhov, R.Z. Sagdeev, Nucl. Fusion Suppl. 2, 465 (1962).

../35

17. K. Appert and J. Vaclavik, Phys. Fluids 22, 454 (1979).

18. K. Appert, T.M. Tran, and J. Vaclavik, Comput. Phys. Commun. 12, 135 (1976).

19. W.E. Drummond and D. Pines, Nucl. Fusion Suppl. 3, 1049 (1962).

20. G. Strang and Q.J. Fix, An Analysis of the Finite Element Method (Prentice-Hall, Englewood Cliffs, 1973).

21. K. Appert, R. Bingham, J. Vaclavik, and E.S. Weibel in 9th European Conference on Controlled Fusion and Plasma Physics (Culham Laboratory, 1979) BP9.

22. G. Vahala and D. Montgomery, J. Pl. Phys. 4, 677 (1970).

23. R.C. Davidson, Methods in Nonlinear Plasma Theory (Academic, New York, 1972).

../36

FIGURE CAPTIONS

Fig. 1 Time evolution of the fluctuation energy, W, and of the ion temperature, T_i, according to the model with Maxwellian distribution functions including resonant (R) or resonant and nonresonant (R + NR) particle interactions.

Fig. 2 Time evolving fluctuation energy, W, ion temperature, T_i, and growth rate ratio, $\langle \gamma_i/\gamma_e \rangle$, according to the models with a Maxwellian (_____) or with a discretized (oooo) ion distribution.

Fig. 3 Typical discretized ion distribution function, $f^{(i)}(v)$, and wave spectrum, $(\omega_k/k = v)$, in the 1D model.

Fig. 4 Time evolution of the fluctuation energy, W, and of the growth rate ratio, $\langle \gamma_i/\gamma_e \rangle$, as obtained with the 1D-2D-2D model.

Fig. 5 Time evolving fluctuation energy, W, electron temperature, T_e, ion to electron temperature ratio, T_i/T_e, and number of trail ions, n_t, according to the 1D model with a discretized ion distribution.

../37

Fig. 6 Fluctuation energy, W, versus the number of tail ions, n_t, in course of time for three different initial fluctuation levels, W(0).

Fig. 7 Typical time evolution of the fluctuation energy, W, and of the electric field, E, as obtained with the extended 1D-2D-2D model where some 2D effects have been included in the 1D ion dynamics.

Fig. 8 The ion distribution function in the resonant region at 5 subsequent times according to the extended 1D-2D-2D model. The arrows point towards the values of c_s at these times.

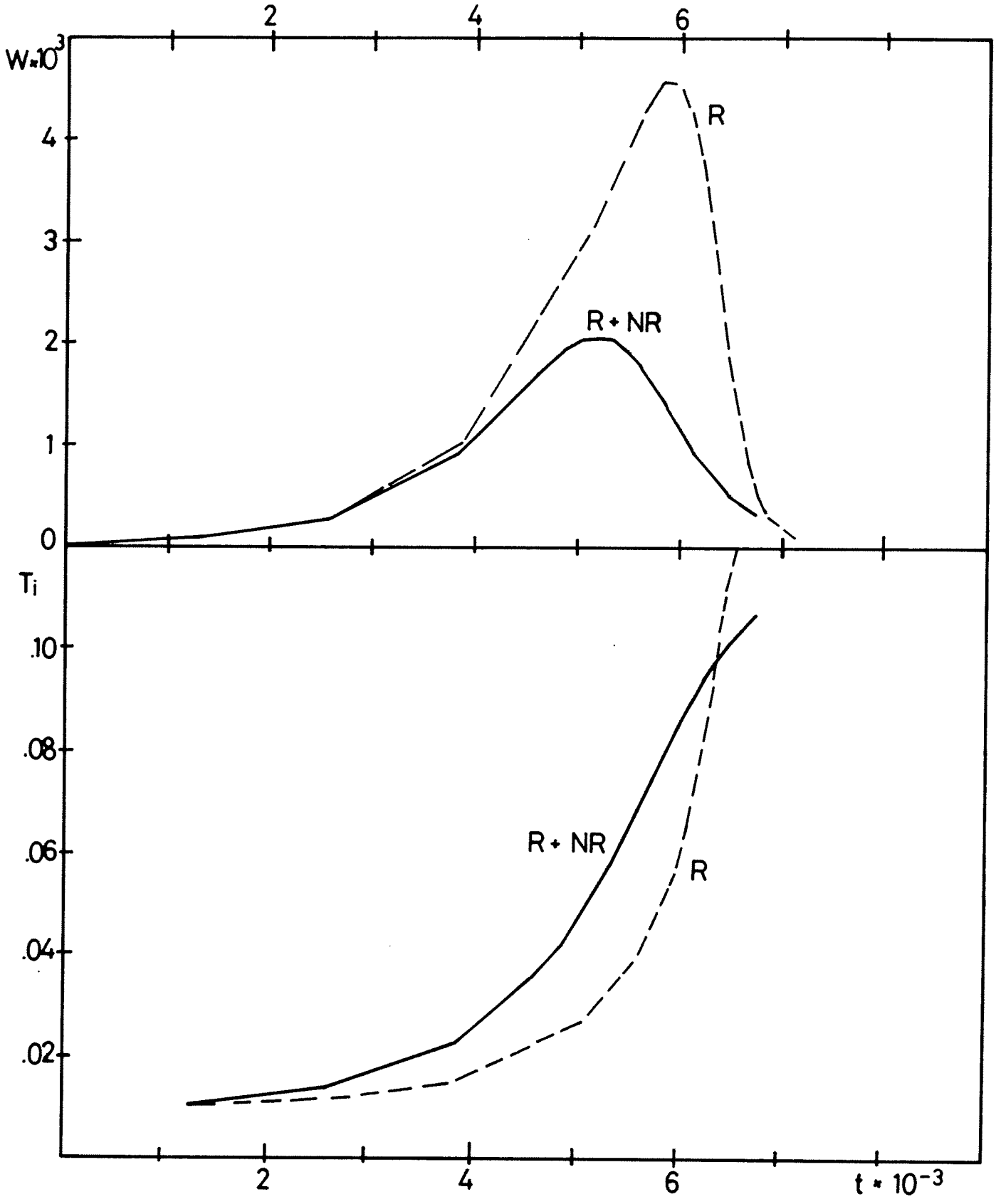

FIG.1

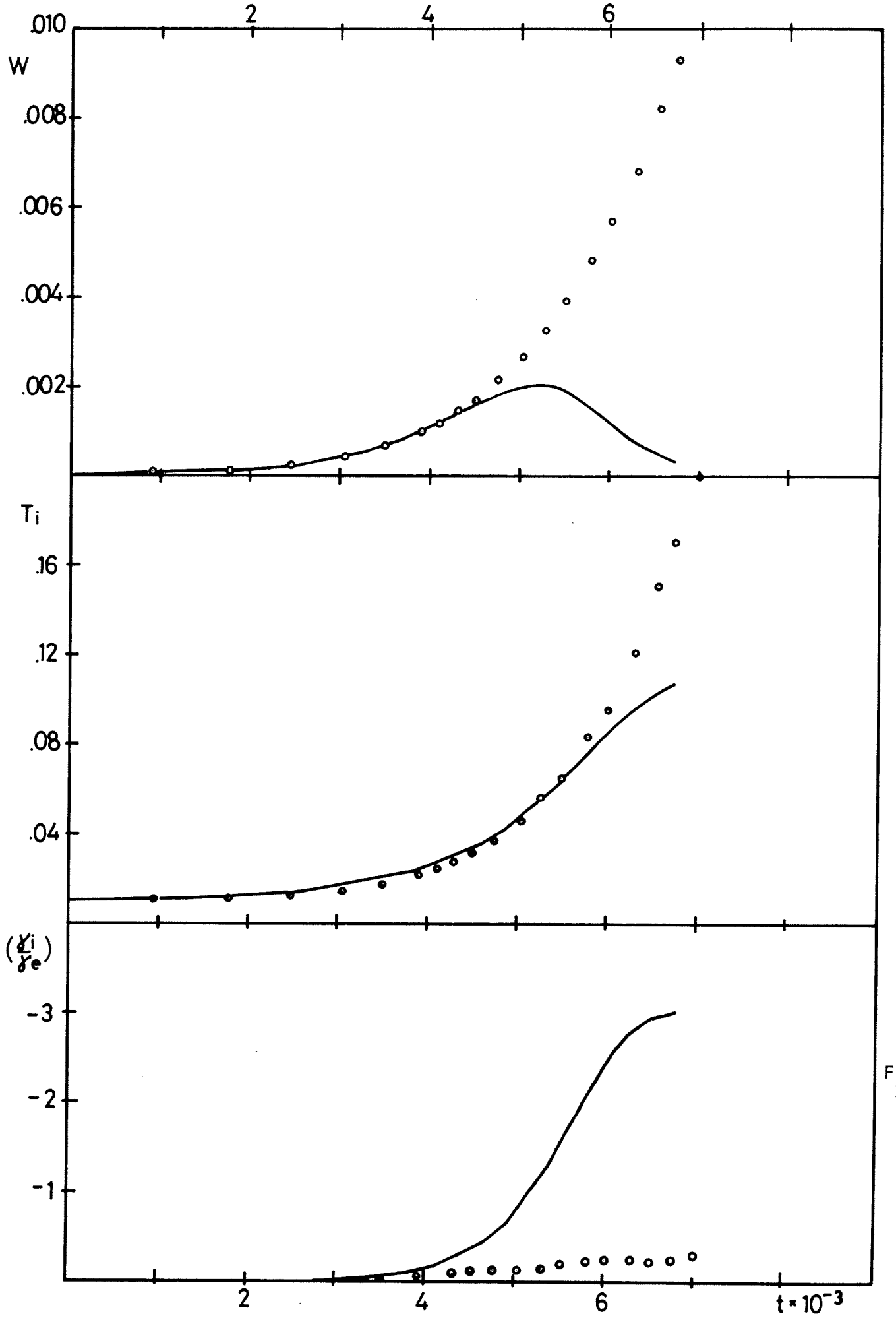
.010
.008
.006
.004
.002
W
2
4
6
T_i
.16
.12
.08
.04
$(\frac{\gamma_i}{\gamma_e})$
-3
-2
-1
2
4
6
$t \times 10^{-3}$

FIG. 2

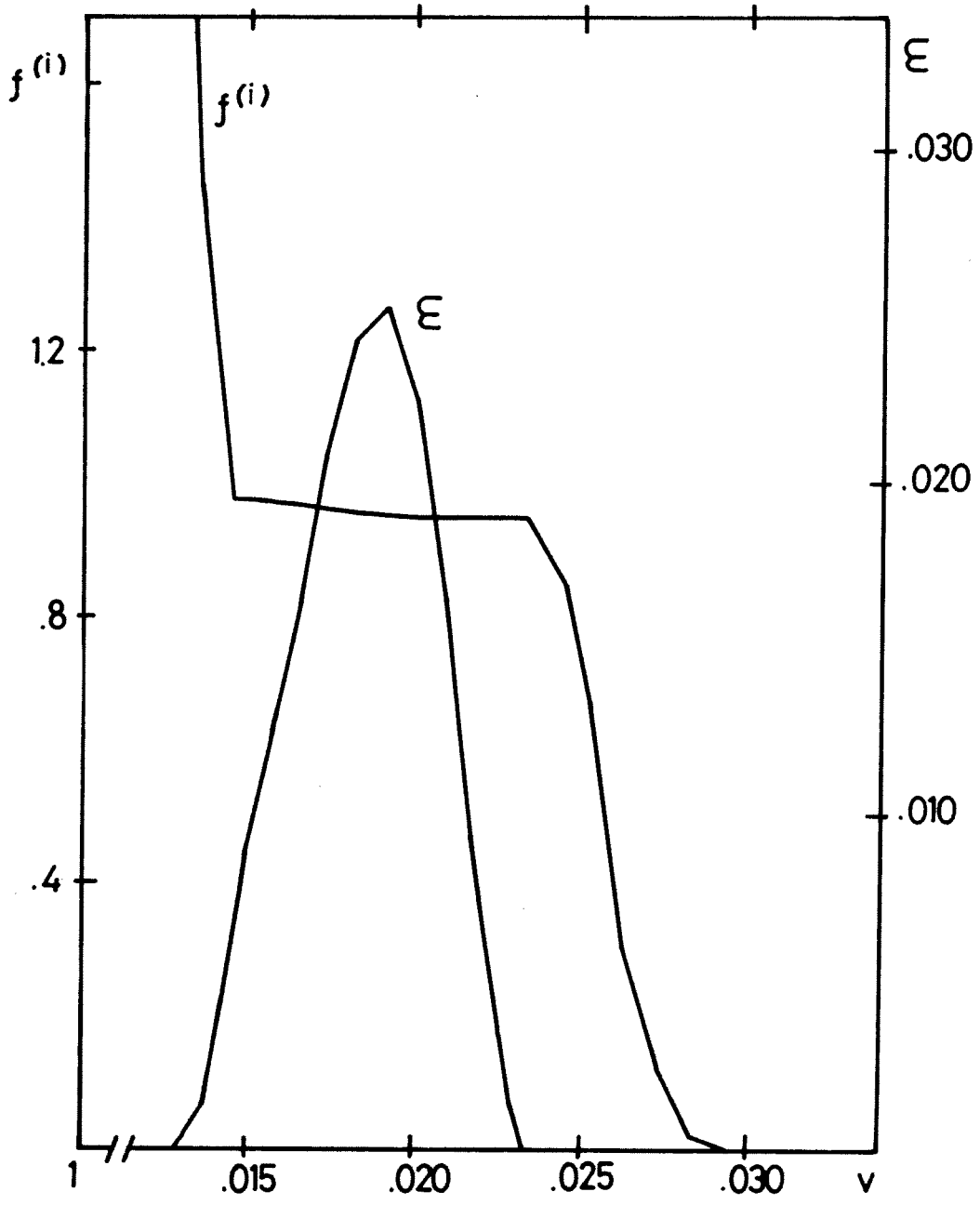

FIG.3

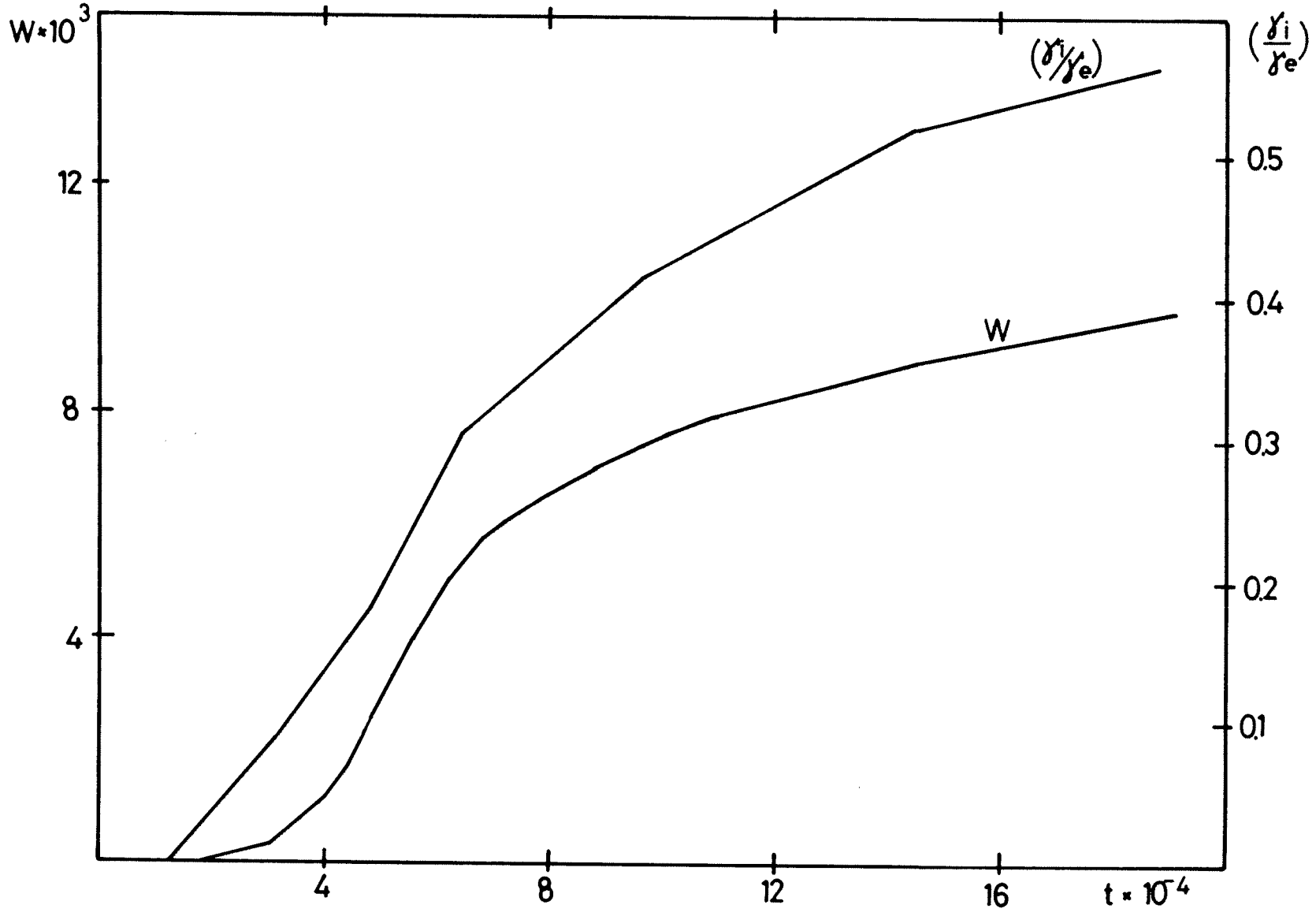

FIG.4

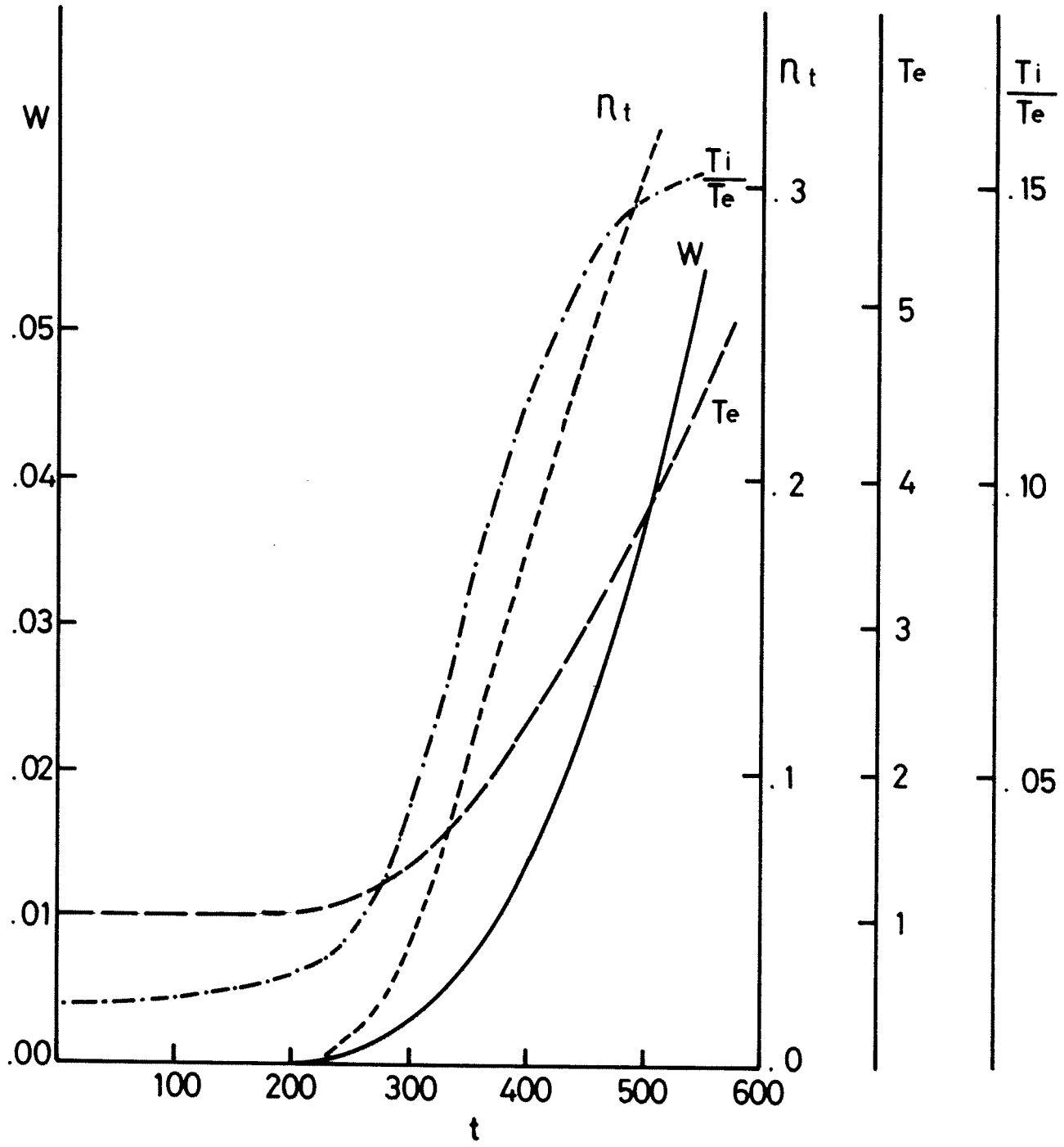
W
.05
.04
.03
.02
.01
.00
100
200
300
400
500
600
t
n_t
n_t
$\frac{Ti}{Te}$
W
Te
.3
.2
.1
.0
Te
5
4
3
2
1
$\frac{Ti}{Te}$
.15
.10
.05

FIG.5

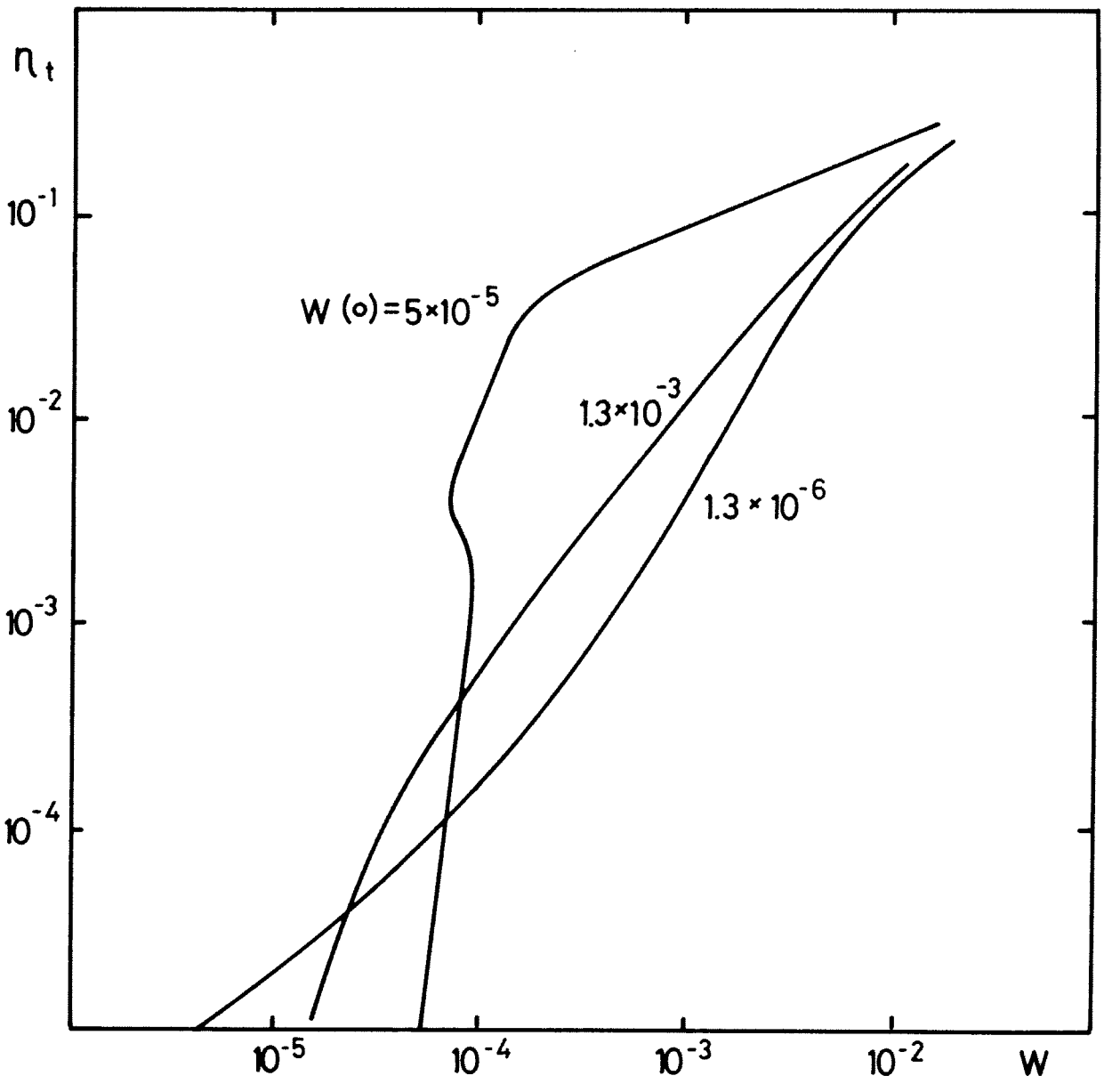

FIG.6

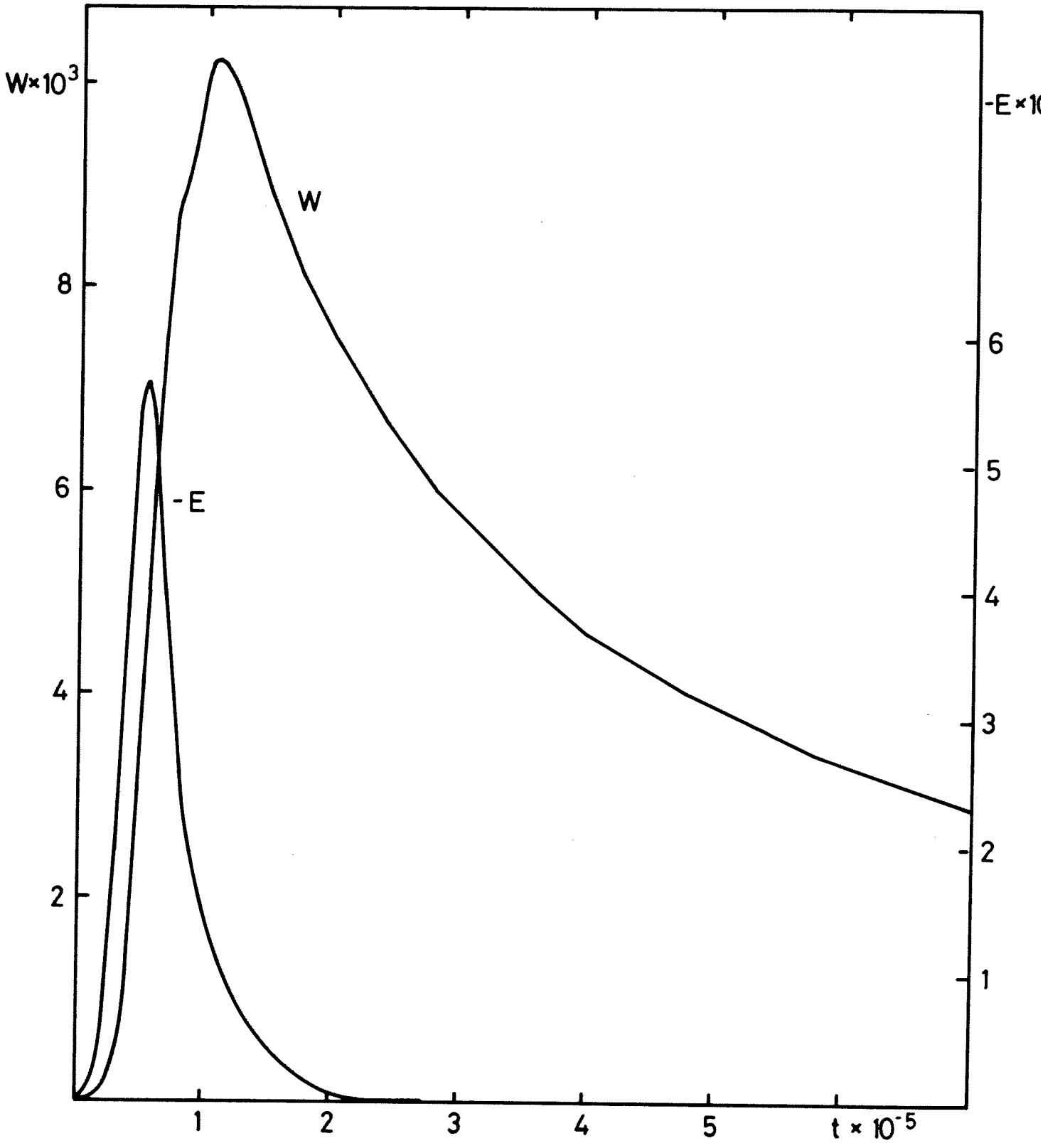

FIG.7

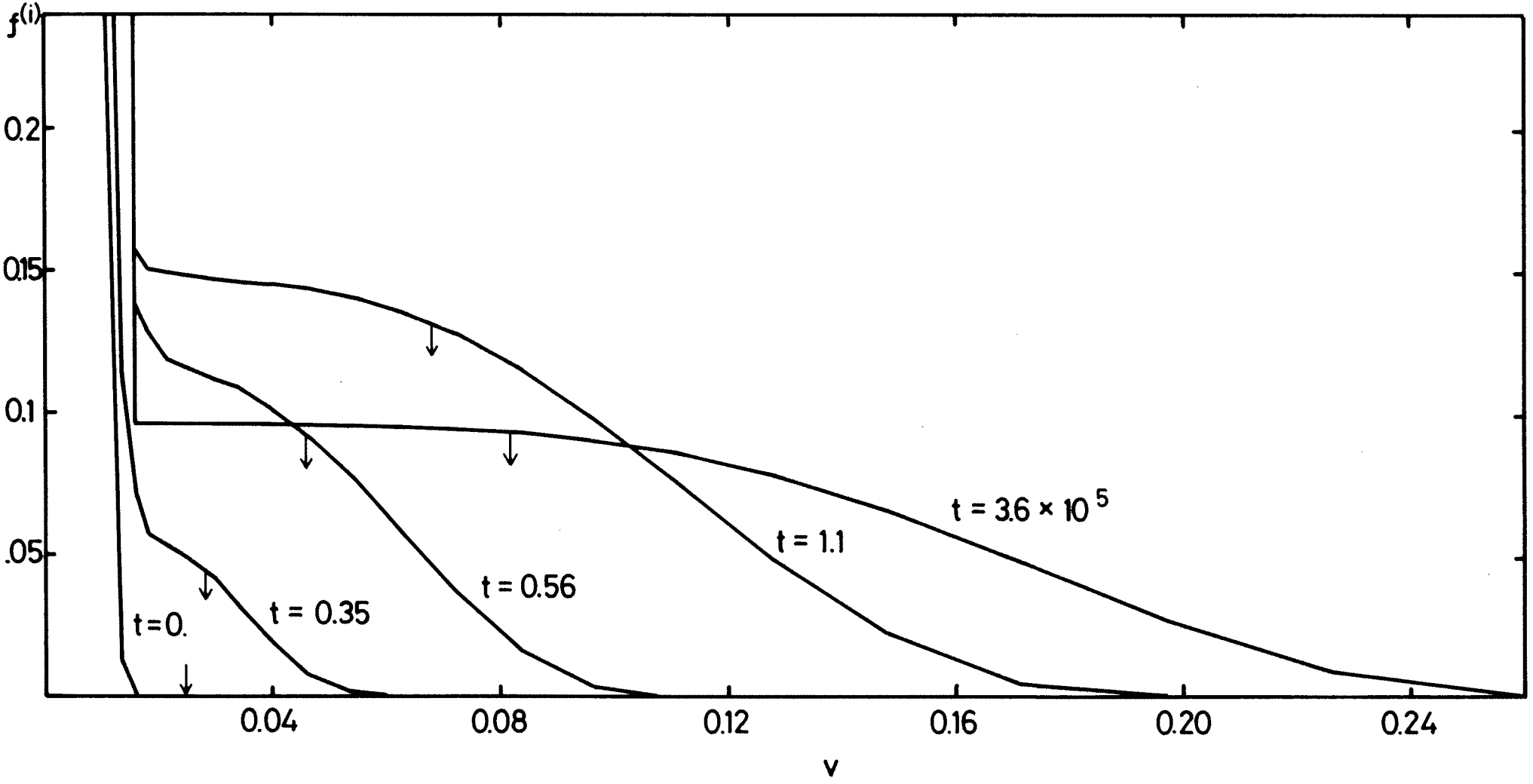

FIG.8